Agnieszka Zuber, Malcolm Purdey, Erik Schartner, Caroline Forbes, Benjamin van der Hoek, David Giles, Andrew Abell, Tanya Monro, Heike Ebendorff-Heidepriem
Detection of gold nanoparticles with different sizes using absorption and fluorescence based method
Sensors and Actuators, B: Chemical, 2016; 227:117-127

Originally published at:
http://doi.org/10.1016/j.snb.2015.12.044

Sensors and Actuators B 227 (2016) 117–127

Contents lists available at ScienceDirect

Sensors and Actuators B: Chemical

journal homepage: www.elsevier.com/locate/snb

Detection of gold nanoparticles with different sizes using absorption and fluorescence based method

Agnieszka Zuber[a,c,*], Malcolm Purdey[a,b], Erik Schartner[a,b], Caroline Forbes[c], Benjamin van der Hoek[c], David Giles[c], Andrew Abell[a,b], Tanya Monro[a,b,d], Heike Ebendorff-Heidepriem[a,b,c]

[a] Institute for Photonics and Advanced Sensing, School of Physical Sciences, The University of Adelaide, Adelaide 5005, SA, Australia
[b] ARC Centre of Excellence for Nanoscale BioPhotonics, The University of Adelaide, Adelaide 5005, SA, Australia
[c] Deep Exploration Technologies Cooperative Research Centre, School of Physical Sciences, The University of Adelaide, Adelaide 5005, SA, Australia
[d] University of South Australia, Adelaide 5000, SA, Australia

ARTICLE INFO

Article history:
Received 26 August 2015
Received in revised form 2 December 2015
Accepted 12 December 2015
Available online 17 December 2015

Keywords:
Gold nanoparticles
Absorption
Fluorescence
BODIPY
Optical fibre
LOQ

ABSTRACT

Growing world demand for gold and decreasing discovery rates of ore deposits necessitates new techniques for gold exploration. Current techniques for the detection of ppb level of gold, such as inductively coupled plasma mass spectrometry (ICP-MS) are not field-deployable. By contrast, current portable device such as X-ray fluorescence (XRF) based sensors are not sufficiently sensitive. Thus, there is growing interest in developing a new, easy-to-use and fast method for detection of low concentrations of gold at the site of an exploration drilling rig.

Two optical methods, absorption and fluorescence, are examined for their suitability for low gold concentration detection. Absorption study is based on the analysis of localised surface plasmon resonance peak. For fluorescence analysis, the ability of gold nanoparticles to specifically catalyse the conversion of the non-fluorescent compound (I-BODIPY) to the fluorescent derivative (H-BODIPY) is used. For both absorption and fluorescence methods, the limit of quantification (LOQ) of gold nanoparticles (NPs) was found to be dependent on the NP size (71 ppb of 5 nm and 24.5 ppb of 50 nm NPs for absorption and 74 ppb of 5 nm and 1200 ppb of 50 nm NPs for fluorescence). The LOQ for fluorescence for 50 nm NPs measured in a suspended core optical fibre was almost twice lower than in a cuvette. The field deployment potential of these methods was also determined using a portable set up.

1. Introduction

Gold is utilised in everyday life from jewellery, through electronics, to drug delivery. Global consumer demand for this precious metal is increasing, and in 2013 it reached above 4000 t per year [1]. The major consumers are China and India, demanding 1275 t and 975 t in 2013, respectively [2]. However, the global discovery rate of gold (and other) deposits is rapidly declining [3], which is primarily a function of ore deposits exposed at the Earth's surface already being found, and undiscovered deposits being buried by younger rock sequences [3,4]. Thus, new techniques are required to explore for ore deposits, which in turn calls for the need to be able to quickly obtain geochemical analysis of rock samples, and the ability to detect economic elements such as gold at lower concentrations [4].

An alternative method for gold exploration is to analyse the concentration of gold in the regolith [5], as well as in the leaves and twigs of trees growing in proximity of gold deposits [6]. Geochemical signatures of gold deposits buried to 35 m depth were recognised in plants such as *Eucalyptus* [6]. The gold was first transported in an ionic (Au^{3+}), water soluble form from the roots to the leaves, and then reduced to gold metal nanoparticles (Au^0) and accumulated within the plant cells. Analysing of plant samples implies that no drilling would be required to recognise the signature of a proximal ore deposit. Plants are not the only living organisms capable of accumulating gold. Bacteria such as *Cupriavidus metallidurans* can also take up gold ions and convert them into gold nanoparticles (NPs) [7], which contributes to the formation of gold grains in the soil [8]. The ability to detect low concentrations of gold in the soil could potentially reduce the cost of searching for a new gold ore deposits.

* Corresponding author at: Institute for Photonics and Advanced Sensing, The University of Adelaide, North Terrace Campus, The Braggs L1.81, Adelaide 5005, SA, Australia. Tel.: +61 8831 32325.
E-mail address: agnieszka.zuber@adelaide.edu.au (A. Zuber).

http://dx.doi.org/10.1016/j.snb.2015.12.044

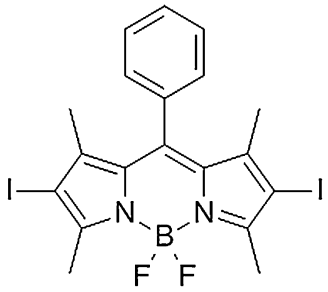

Fig. 1. Structure of bisiodinated derivative of 4,4-difluoro-4-bora-3a, 4a-diaza-*s*-indacene (I-BODIPY).

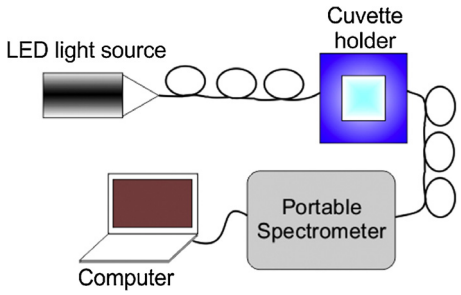

Fig. 3. Sketch of the in-house optical set-up with portable spectrometer used for absorption measurements.

In addition to the potential benefits for ore exploration, detection of low levels of gold would be advantageous for biomedical and environmental research. Gold NPs conjugated with antibodies are used for drug delivery [9,10] and sensing [11] applications. Gold NPs are also employed for gene therapy [12] and gene specific sequence sensing [13]. Photostability makes NPs a competitive staining method in cellular imaging, where the gold NPs conjugated to a cell binding ligand are visible as the bright spots in a dark field image [14]. Analysis of the concentration of NPs in bioconjugates would enable sensing of low concentrations of biomolecules using well-established spectrophotometer or fluorometer based methods [11]. Due to the enhanced absorption and scattering compared to bulk gold, nanoparticles are utilised in photothermal cancer therapy [15,16]. The growing biomedical applications of gold NPs demands that their cytotoxicity and safety be established. Cell culture studies indicate that small gold NPs (1–2 nm) are more toxic than larger NPs (15 nm) in fibroblasts, epithelial cells, macrophages and melanoma cells [17,18]. Sensitive methods for the detection of gold NP would facilitate tracking the accumulation of gold NP in cells. The accumulation of gold NPs in rat organs after administration of 0.56 mg of NPs per gram of animal [18] ranged from 0.08 ppb in brain, through 20 ppb in muscle and 30 ppb in bone to 260 ppb in blood. Analysis of accumulation of gold NPs conjugated with the antibody against specific protein could allow fast diagnosis of carcinogenesis, Alzheimer disease or Parkinson's disease. Sensing of gold NPs released into air and water would monitor the uncontrolled release of particles into the environment and increase safety related to the handling of NPs [19].

Similar detection limits as for medical diagnosis are required for gold exploration purpose. The average crustal abundance of gold is 1.3 ppb [20]. Anomalous gold concentrations can be between 0.5 and 8 ppm [21,22]. Therefore, detecting anomalous levels of gold requires instrumentation with low detection limits. Currently, the analysis of gold in a rock sample at a drill rig may be performed using portable XRF, but the detection limit of this technique is high in the order of few ppm [23]. In addition, the signal of gold often overlaps with tungsten commonly used in drill bits thus, these techniques do not allow an analysis of the presence of gold in the drilling sample at sufficiently low levels to explore for new ore deposits.

One of the methods for sensitive detection of gold is inductively coupled plasma mass spectroscopy (ICP-MS) with detection of ppt level of gold in both geological [24,25] and biological samples [18]. Another method is inductively coupled plasma atomic emission spectroscopy (ICP-AES) with detection limits as low as 1 ppb [26]. However, detection at these levels requires the rock to be crushed and fire assays to be performed to remove other elements and then aqua regia and cyanide digestion to leach gold from the sample. This analysis process can take days and requires samples to be transported to a laboratory. In addition, the required instruments are not compatible with on-site analysis at the drill rig. This is a major issue why on-site analysis for fast detection of gold during drilling is of growing interest to gold exploration companies, demanding the development of a portable sensing method for low level gold detection at the site of the drilling rig.

The research presented here focuses on the use of optical methods, such as absorption and fluorescence, for detection of gold nanoparticles at concentrations of ppb order. Gold NPs have unique optical properties such as localised surface plasmon resonance (SPR) [27], plasmon resonance scattering [27] and a catalytic effect on fluorophores [28] which can be utilised for sensing purposes.

SPR is the collective oscillation of electrons on the surface of metal excited by photons, which results in a peak observed in the absorption spectrum of a sample. The position and width of the SPR absorption peak depends on the size and agglomeration of the gold

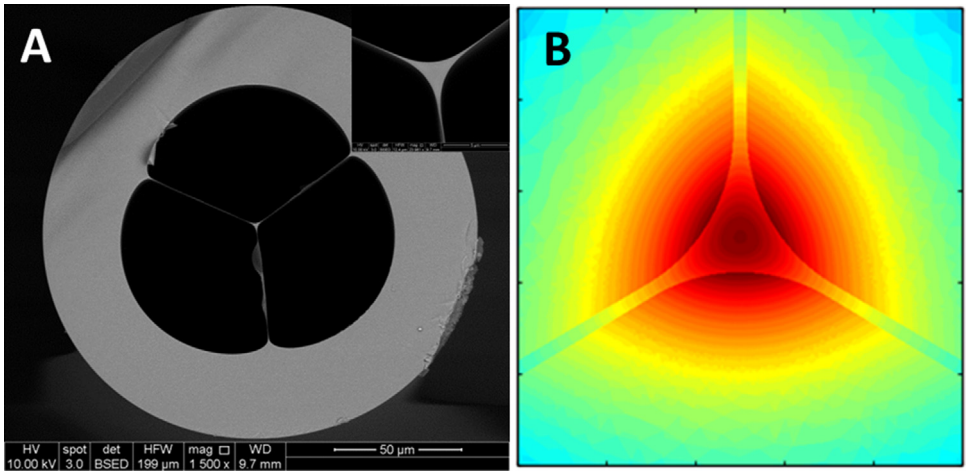

Fig. 2. (A) Cross-sectional image of the suspended core fibre used (inset showing magnified image of the fibre core), (B) example of a core of a suspended core fibre indicating the intensity of the evanescent field in the holes surrounding the solid core with high intensity marked red and low intensity marked blue.

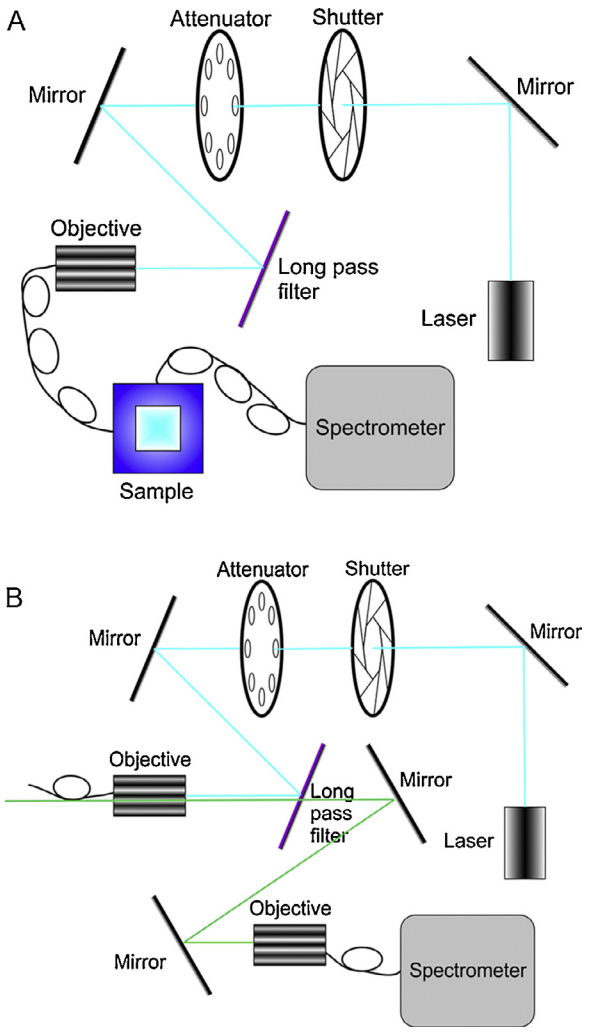

Fig. 4. Optical set-up for the measurement of the fluorescence of BODIPY in the presence of gold NPs in (A) cuvette and (B) SCF. M-mirror, DC-dichromic mirror.

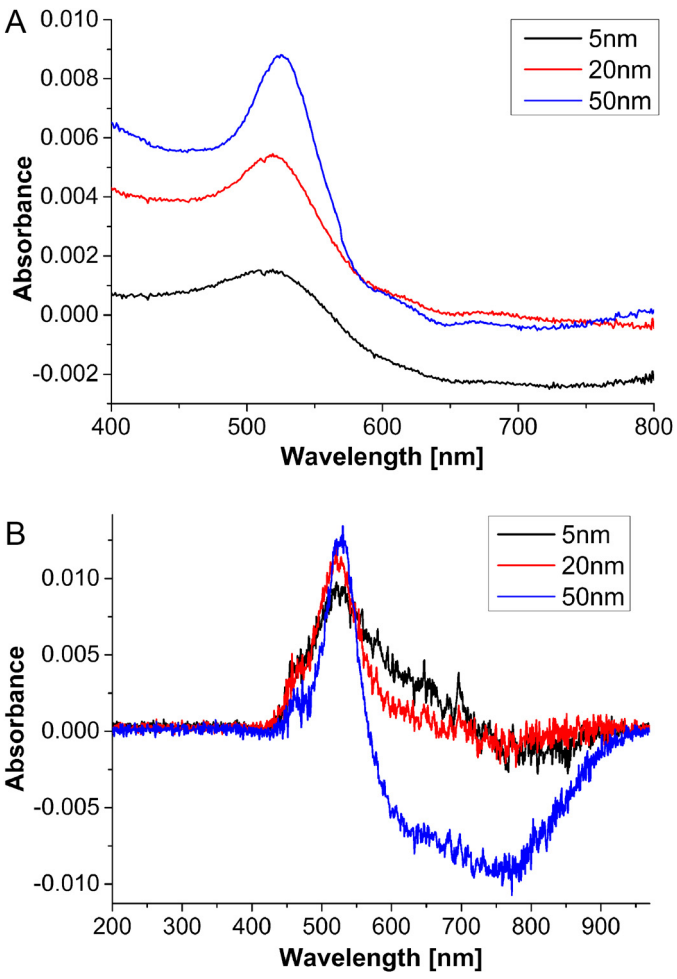

Fig. 5. Absorption spectrum of 5 nm, 20 nm and 50 nm gold NP solutions in cuvette: (A) for 236 ppb of gold and using laboratory Cary spectrometer, (B) for 738 ppb of gold and using portable spectrometer.

NPs. A shift to longer wavelengths and broadening of the SPR peak is observed as the size of NPs increases and as the distance between particles decreases due to aggregation [29]. The intensity of the SPR peak is related to the concentration of gold NPs. Thus, combining peak wavelength, broadening and intensity of the SPR peak allows determination of the size related detection limit of gold NPs. Zeng et al. [30] observed enhanced SPR peak intensity for smaller nanoparticles (40 nm) compared to larger ones (80 nm). The impact of the size and shape of gold NPs on the extinction coefficient of the SPR peak has been investigated [31–33]. However, to the best of our knowledge, the LOQ for gold NPs using the absorption method has not been determined. Also, the impact of the NP size on LOQ that can be achieved using this technique has not been explored. In addition, all the measurements to date were done with laboratory based spectrometers, which limits the applicability of the method. Here we examine the LOQ that can be achieved using both large, laboratory-based and hand-held, portable spectrometers. The use of portable spectrometer allows the method to be employed in the field and thus opens up possibility for new applications.

Another property of gold NPs that is promising for sensing application is fluorescence enhancement due to catalytic reaction. The fluorophore, a bisiodinated derivative of BODIPY (4,4-difluoro-4-bora-3a, 4a-diaza-*s*-indacene) (I-BODIPY) was found to show specific reactivity towards gold NPs [28]. Fluorescence is observed as a result of the catalytical change of non-fluorescent I-BODIPY to fluorescent H-BODIPY. Here we determined for the first time the dependence of LOQ on the size of NPs using BODIPY as a sensing molecule. Choosing a right derivative of the fluorophore and using a portable spectrometer and water as a solvent can decrease the LOQ significantly and broadens the applications of this method beyond the laboratory including not only mining, but also biological applications.

Optical fibres demonstrate growing interest for sensing applications [34–36]. In this work we use a microstructured optical fibre consisting of a solid glass core surrounded by three air holes (hereafter referred to as suspended core fibre (SCF)). In this fibre type, part of the light guided along the fibre core is located outside of the glass core and in the air holes, commonly referred to as the evanescent field. The portion of the light located in the air holes can be used for light-matter-interaction, and hence sensing of an analyte situated in the holes. SCFs offer a range of advantages for sensing applications, including the analysis in a SCF requires only small sample (nanolitre volumes) [37]; sensing with a SCF can be made highly specific by binding specific functional groups on the surface of the fibre core [38]; and due to their compact size, SCFs are particularly suitable for portable devices. SCFs are also useful for remote measurements, such as downhole sensing in a drilling rig.

In this paper, we investigate the viability of absorption and fluorescence methods for detection of ppb concentrations of gold NPs and the impact of the size of NPs on the LOQ. As sensing with a SCF may achieve lower detection limit compared to a cuvette depend-

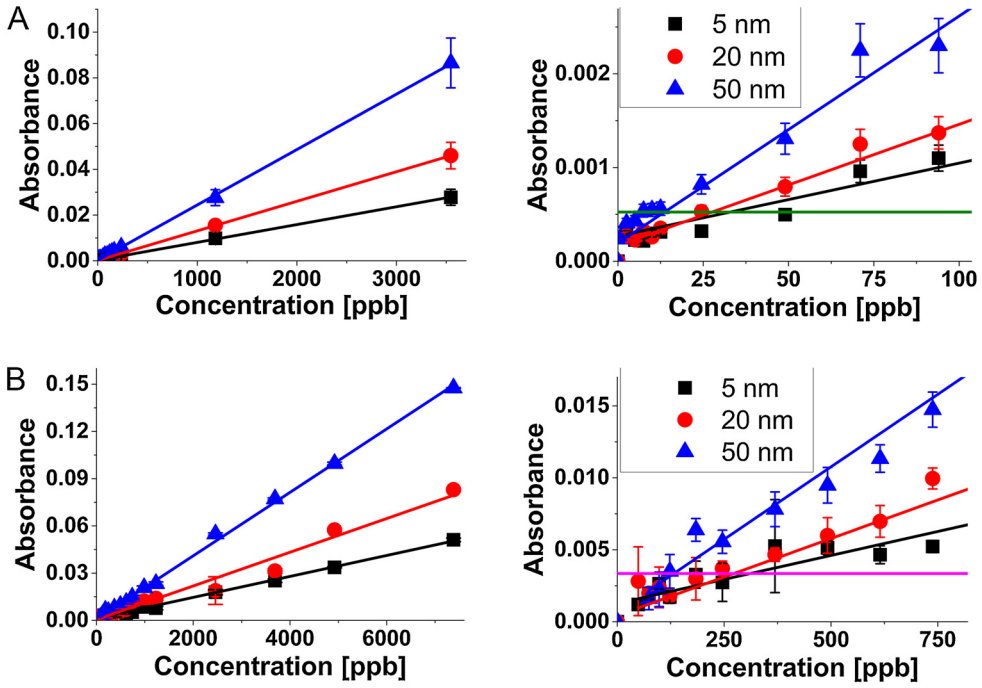

Fig. 6. Linear regression of the peak absorbance as a function of gold concentration for 5 nm, 20 nm and 50 nm gold NP solutions in cuvette: (A) using laboratory Cary spectrometer (R^2 = 0.999 for all analysed sizes) (green line in the insert showing LOQ), (B) using portable spectrometer (R^2 = 0.996, 0.976, 0.998 for 5, 20 and 50 nm gold NPs, respectively) (pink line in the insert showing LOQ).(For interpretation of the references to colour in this figure legend, the reader is referred to the web version of this article.)

ing on the measurement method and the fibre core size [39], we investigate whether use of a SCF can yield lower detection limits for gold NPs compared to measurement in a cuvette. We then compare the detection limits and field deployment ability of the two detection methods in cuvette and SCF using laboratory-based and portable spectrometers.

2. Methods

2.1. Gold nanoparticles

Commercially available, monodisperse gold NPs in three different sizes (4.8 ± 0.7 nm, 20 ± 2.5 nm and 51 ± 6.1 nm diameter, hereafter referred to as 5 nm, 20 nm and 50 nm NPs) were acquired from Nanocomposix. The initial concentration of the NPs in 2 mM sodium citrate solution was 0.25 mM. A range of concentrations was prepared by adding NP solution to water with a final volume of 2 mL.

In this paper, the following gold concentrations are used:

- Ratio of weight of gold to weight of sample in parts per billion (ppb), where 1 ppb equals 1 μg of gold in 1 kg of sample
- Molar concentration of gold NPs in mol of gold NPs per litre of sample

Assuming that the gold NPs were spherical in shape and their density being the same as bulk gold (i.e. 19.3 g/cm^3), the concentration of gold NPs was calculated using

$$C_s = 6 * \left(\frac{C_{Au} * M_{Au}}{\pi * \rho_{Au} * D_s^3} \right) * \frac{1}{N_A} \quad (1)$$

where C_s is the molar concentration of gold NPs, C_{Au} is the molar concentration of gold atoms/ions, M_{Au} is the molecular weight of gold, ρ_{Au} is the density of gold, D_s is the diameter of the gold NPs, and N_A is the Avogadro constant.

2.2. Synthesis of I-BODIPY

The fluorophore I-BODIPY was synthesised by reaction of H-BODIPY with iodine. Specifically H-BODIPY (25 mg, 0.08 mmol) was suspended in methanol (10 mL) and I_2 (54 mg, 0.20 mmol) was added whilst stirring. A solution of HIO_3 (30 mg, 0.16 mmol) in water (200 μL) was added dropwise over 5 min. The reaction mixture was stirred at 25 °C for 30 min and the solution turned a deep fluorescent red/brown colour. The solvent was removed under reduced pressure and the compound was eluted through a silica column with 5: 1 petroleum ether: chloroform to give I-BODIPY as a dark red solid (21 mg, 46%) ^{1}HNMR ($CDCl_3$): 7.53–7.49 (3*H*, m), 7.26–7.24 (2*H*, m), 2.65 (6*H*, s), 1.38 (6*H*, s) [13]CNMR ($CDCl_3$): 156.8, 145.4, 141.4, 134.7, 131.3, 129.5, 129.4, 127.8, 85.65, 16.9, 16.0

Using NMR (Supplementary data), the structure of the synthesised I-BODIPY was determined (Fig. 1) in accordance with literature [40].

The structure of the fluorophore presented here differs from that one presented by Park et al. [28] through the absence of two polyethyl ether groups on the phenyl ring. For the sensing experiments, I-BODIPY was first dissolved in dimethyl sulfoxide and then diluted in aqueous solution.

2.3. Fibre

The SCF made from silica was used for the fibre experiments since it provides several advantages for sensing applications. Silica is made in ultrahigh purity enabling low fibre loss and thus use of long fibre length; the high thermal, mechanical and corrosion stability of silica allows use in harsh environments; and the relatively low refractive index of silica (1.45 in the visible) leads to larger fraction of light being located in the air holes, enabling higher sensitivity [41].

The power fraction of light in the air holes increases with decreasing core size, and hence, the sensitivity of a SCF increases

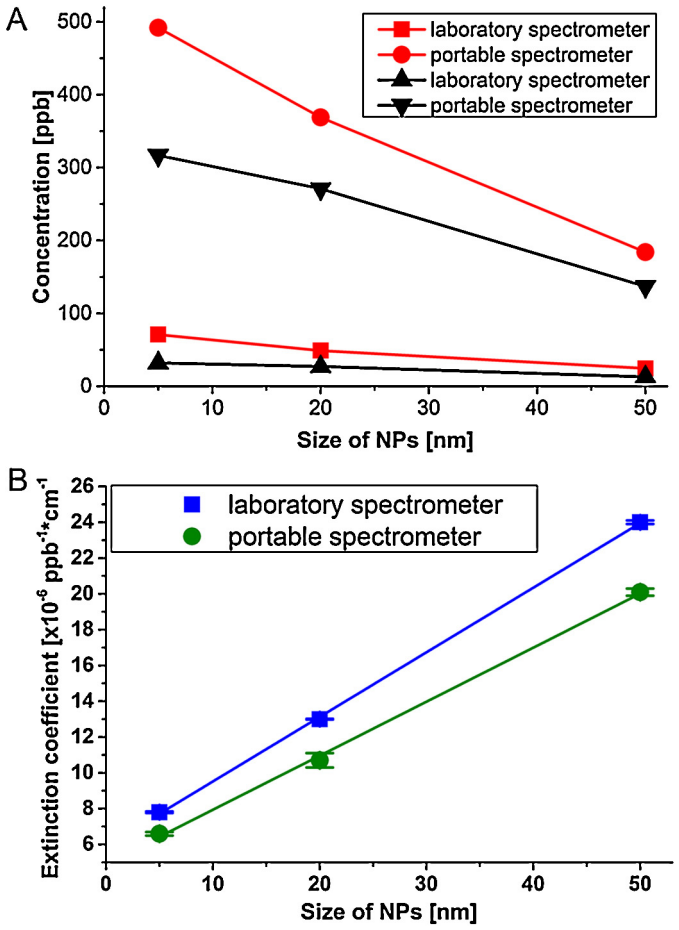

Fig. 7. (A) Experimental LOQ of absorption measurement of gold NPs using laboratory and portable spectrometer (red) compared with theoretical values (black). (B) Linear regression of extinction coefficient as a function of gold NP size measured using laboratory spectrometer ($R^2 = 0.999$) and portable spectrometer ($R^2 = 0.998$).(For interpretation of the references to colour in this figure legend, the reader is referred to the web version of this article.)

with decreasing core size [42]. Therefore, a SCF was used with small core diameter of 1.5 μm with a cross-sectional structure shown in Fig. 2A. The fraction of light being guided in the holes for sensing is schematically shown in Fig. 2B (example only, no actual calculations of the intensity range). The fibre core is surrounded by three holes of 60 μm diameter. The large hole size prevents hole blockage by particles present in a liquid, as well as reducing the required time to fill the fibre holes.

For the sensing experiments, the fibre was mounted on a 3-axis stage and light was coupled into the core until maximal power at the end of the fibre was measured with a power meter. 50 cm lengths of fibre were used for each experiment. The tip of the fibre was dipped in the gold NPs–BODIPY solution resulting in a 3.7 ± 0.5 cm length of filled fibre (0.3 μL).

2.4. Absorption

The absorbance spectrum of gold NPs was measured using plastic cuvettes and a laboratory-based, commercial instrument or a portable, in-house set-up. A new cuvette was used for each measurement. The absorbance spectrum of water was subtracted from all measured spectra. The commercial instrument used was a UV–vis-NIR spectrometer Cary 5000 (Agilent Technologies). This instrument is hereafter referred to as laboratory Cary spectrometer. The in-house set-up (Fig. 3) consisted of a broadband LED light source and a portable Ocean Optics QE 65,000 spectrometer, both fibre coupled to a cuvette holder, ensuring the same measurement conditions for each sample. For the laboratory Cary spectrometer, the absorbance was measured directly. For the in-house set-up with portable spectrometer, the transmitted light was recorded using the portable spectrometer and the absorbance was calculated as $-\log_{10}$(intensity of a sample/intensity of water), where intensity refers to the transmitted power measured.

2.5. Fluorescence

The fluorescence of BODIPY solutions was measured using a 473 nm laser light in optical set-ups shown in Fig. 4. The fluorescence was measured in a cuvette (Fig. 4A) and a SCF (Fig. 4B). For cuvette measurements the light was focussed with a 60× objective onto a 200 μm core UV–vis optical fibre (Ocean Optics) that was connected to the cuvette holder, thereby guiding the light to the cuvette situated in the holder (Ocean Optics). The emitted light (perpendicular to the excitation light) was collected by a 200 μm multimode fibre (Thorlabs) connected to both the cuvette holder and the spectrometer. For the SCF measurement, the light focussed with the 60× objective was coupled into the core of the SCF. Back propagating emission light passed through the 60× objective, reflected from the mirrors and was coupled by 10× objective into the 200 μm multimode fibre (Thor labs), which guided the collected emission light into the spectrometer.

In order to compare the achievable detection limits with different spectrometers, either a laboratory-based, non-portable spectrometer iHR320 (Horiba Jobin Yvon) (hereafter referred to as laboratory Horiba spectrometer) or a portable Ocean Optics QE65000 spectrometer was used for cuvette and SCF measurements. Note that for absorption and fluorescence measurements, the same portable spectrometer was used, but different laboratory-based spectrometers (Cary 5000 and iHR320, respectively).

For cuvette measurements, the fluorescence of BODIPY was measured using a 473 nm laser with 8 mW output power and an exposure time of 4 s. For SCF measurements, the laser power was decreased to yield similar signal intensity to that of the cuvette results. I-BODIPY was added in a 1:1 ratio into the aqueous solutions of NP. The spectrum of the blank sample (solution of I-BODIPY with no NPs) was subtracted from all spectra measured for samples containing NPs.

2.6. Quantification limit

The limit of quantification (LOQ) was used as a measure for the minimum quantifiable concentration [43], and is defined as

$$\mathrm{LOQ} = \mathrm{mean}_{\mathrm{blank}} + 10 \times \mathrm{SD}_{\mathrm{blank}} \quad (2)$$

where $\mathrm{mean}_{\mathrm{blank}}$ is the mean of the blank sample and SD is the standard deviation of the blank sample [44], which was water for absorption and fluorophore in water for fluorescence measurement. The experimental LOQ is the lowest gold concentration used for which the absorption or fluorescence intensity including error is higher than the LOQ value. The theoretical LOQ is the gold concentration value at which the corresponding absorption and fluorescence intensity is equal to the LOQ value; the gold concentration is calculated using the linear regression of the concentration dependence of the absorption or fluorescence intensity.

3. Results and discussion

3.1. Absorption measurement of gold NPs in a cuvette

Fig. 5A shows the characteristic absorption spectrum related to the surface plasmon resonance (SPR) of 5 nm, 20 nm and 50 nm

Table 1
Extinction coefficient for different sizes of NPs relative to gold concentration (in ppb) and molar gold NP concentration (in mol/L).

Size of NPs	Extinction coefficient determined using laboratory spectrometer: (a) NP concentration in mol/L (b) Gold concentration in ppb	Extinction coefficient determined using portable spectrometer: (a) NP concentration in mol/L (b) Gold concentration in ppb	Extinction coefficient published in the literature: (a) NP concentration in mol/L
5 nm	(a) $5.9 \pm 0.04 \times 106$ L/(mol cm) (b) $7.8 \pm 0.04 \times 10^{-6}$/(ppb cm)	(a) $5.1 \pm 0.08 \times 10^{6}$ L/(mol cm) (b) $6.6 \pm 0.1 \times 10^{-6}$/(ppb cm)	(a) 8.6×106 L/(mol cm) [33] (a) 7.2×106 L/(mol cm) [32]
20 nm	(a) $6.3 \pm 0.01 \times 108$ L/(mol cm) (b) $1.3 \pm 0.002 \times 10^{-5}$/(ppb cm)	(a) $5.2 \pm 0.2 \times 108$ L/(mol cm) (b) $1.07 \pm 0.04 \times 10^{-5}$/(ppb cm)	(a) 8.78×108 L/(mol cm) [33] (a) 5.4×108 L/(mol cm) [32]
50 nm	(a) $1.8 \pm 0.008 \times 10^{10}$ L/(mol cm) (b) $2.4 \pm 0.01 \times 10^{-5}$/(ppb cm)	(a) $1.5 \pm 0.02 \times 1010$ L/(mol cm) (b) $2.01 \pm 0.02 \times 10^{-5}$/(ppb cm)	(a) 1.0×10^{10} L/(mol cm) [32] (a) 0.8×10^{10} L/(mol cm)* [31]

* Measured for 40 nm gold NPs.

Table 2
The length of the fibre required to measure certain concentration of gold using stationery spectrometer.

	5 nm NPs	20 nm NPs	50 nm NPs
Fibre length required to detect 100 ppb of gold	66 m	39 m	21 m
Gold concentration that can be measured with 1 m fibre length	6600 ppb	3900 ppb	2100 ppb

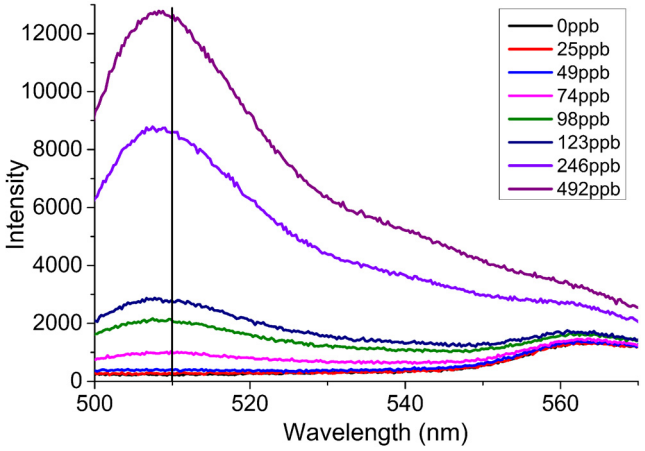

Fig. 8. Fluorescence spectrum measured in cuvette using laboratory spectrometer at 50 min incubation of different concentrations of 5 nm gold NPs in water with 60 nM I-BODIPY. The peak at 510 nm (marked with black line) depends on the gold concentrations used.

gold NPs for the same gold concentration and using laboratory Cary spectrometer. The peak maximum shifted from 514 nm for 5 nm NPs, through 519 nm for 20 nm NPs to 526 nm for 50 nm NPs. SPR peak of NPs made of different metal is shifted significantly, e.g. silver NPs 10–395 nm, 20–400 nm, 50–420 nm [45]. Thus, this method enables selective detection of gold NPs of defined size and shape. Fig. 5B shows the surface plasmon resonance peak of the same NPs using portable spectrometer. The peak maximum shifted from 518 nm for 5 nm NPs, through 520 nm for 20 nm NPs to 527 nm for 50 nm NPs. The shift towards longer wavelengths with increasing NP size is related to the differences in the frequency of surface plasmon oscillations of the free electrons [46]. The increase in absorbance with NP size is attributed to the enhanced mean free path of the electrons in the larger NPs [32]. This increase leads to lower LOQ for larger NPs.

Fig. 6 shows the concentration dependence of the peak absorbance for 5 nm, 20 nm and 50 nm gold NPs in cuvette measured using laboratory Cary spectrometer (Fig. 6A) and portable spectrometer (Fig. 6B). The peak absorption increases linearly with gold concentration, which indicates that gold NPs obey the Lambert-Beer law. This result is consistent with the literature [47]. The experimental LOQ (lowest measured gold concentrations yielding peak absorbance values above the LOQ) are 71 ppb for 5 nm NPs, 49 ppb for 20 nm NPs and 24.5 ppb for 50 nm NPs for the laboratory Cary spectrometer and 492 ppb for 5 nm NPs, 369 ppb for 20 nm NPs and 184 ppb of 50 nm NPs for the portable spectrometer (Fig. 7A). For the laboratory Cary spectrometer, the LOQ decreases by a factor of 10 as the NP sizes increases from 5 nm to 50 nm, while for the portable spectrometer this decrease is a factor of 3. Compared to the laboratory spectrometer, measurements with the portable spectrometer result in an approximately 7 times higher LOQ for all analysed sizes of NPs. This is attributed to differences in the optical set-ups, and is suggested to be related to coupling of the light into the sample and from the sample to the detector, optimised coupling optics and minimal noise due to double Littrow monochromator [21] which enable maximal level of light throughput and thus lower value of LOQ (5.25×10^{-4}) compared to the in-house set-up with portable spectrometer (3.35×10^{-3}).

The theoretical LOQ can be determined from the extinction coefficient. The decadic extinction coefficient (Fig. 7A, Table 1) was determined as the slope of the linear regression of the peak absorbance as a function of gold concentration using the laboratory spectrometer (Fig. 6A) and the portable spectrometer (Fig. 6B). In accordance with the different LOQ values obtained by the two spectrometers used, high certainty in the regression was obtained for data collected with the laboratory spectrometer ($R^2 = 0.999$), whereas larger variation was found for the portable spectrometer ($R^2 = 0.996$ for 5 nm, $R^2 = 0.976$ for 20 nm and $R^2 = 0.998$ for 50 nm NPs). The extinction coefficient increases with the size of the NPs (Fig. 7B) as reported by others [31–33]. This relationship is independent of the capping agent and solvent used for the gold NPs [33]. Using the extinction coefficients, the gold concentrations that yield peak absorbance values equal to LOQ can be calculated. These theoretical values of LOQ are compared with the measured values of LOQ in Fig. 7A. The trends of experimental and theoretical LOQs are similar. However, the difference between the values decreases with increasing size of the NPs. The experimental values measured with the both spectrometer are approximately 1.3–2.2times higher than theoretical values. The discrepancy between theoretical and experimental values is related to fewer number of data points measured as well as included error bars for the determination of the experimental LOQ.

The extinction coefficient values shown in Fig. 7B were calculated for the concentration of gold in ppb. Note that other papers [32,33] report molar concentration of gold NPs. In order to compare the extinction coefficient values measured in this work with those reported in the literature, we also calculated the extinction coefficients for molar concentration of gold NPs. The values

Table 3
Summary of LOQs achievable with different methods for gold concentration (ppb) and NP concentration (pM).

Method	Sample container type	NP diameter (nm)	Spectrometer	Theoretical LOQ of gold concentration (ppb)	Experimental LOQ of gold concentration (ppb)	Experimental LOQ of NP concentration (pM)
Absorption	Cuvette	5	Laboratory Cary	32	71	93
			Portable	310	492	647
		20	Laboratory Cary	27	49	1.0
			Portable	271	369	7.58
		50	Laboratory Cary	14	24.5	0.03
			Portable	132	184	0.24
Fluorescence	Cuvette	5	Laboratory Horiba	50	74	97.3
			Portable	64	74	97.3
		20	Laboratory Horiba	260	369	7.6
			Portable	369	492	10.1
		50	Laboratory Horiba	1020	1200	1.6
			Portable	674	1200	1.6
Fluorescence	Fibre	5	Laboratory Horiba	28	74	97.3
			Portable	39	74	97.3
		20	Laboratory Horiba	338	492	10.1
			Portable	168	246	5.05
		50	Laboratory Horiba	45	738	0.97
			Portable	140	492	0.65

of extinction coefficient of gold NPs [L/(mol cm)] reported here for the two different types of spectrometers are similar, and they are in the same order of magnitude to those reported in the literature [31–33].

3.2. Absorption measurement of gold NPs in suspended core fibre

Considering the best case scenario of 100% coupling efficiency and negligible fibre loss, the fibre length (d) necessary to measure a given peak absorbance value of gold NPs can be calculated based on the Beer–Lambert law: [48]

$$d = \frac{A * \ln 10}{\varepsilon * C * \Phi} \quad (3)$$

where A is the peak absorbance, ε is the decadic extinction coefficient, C is the gold concentration and Φ is the power fraction of light in the sample (i.e. in the filled holes in the case of SCF). Alternatively, Eq. (3) can be used to calculate the concentration that can be measured at the detection limit for a certain fibre length. The extinction coefficients determined for the cuvette measurements using a laboratory spectrometer (Table 1) were used for the calculations. The power fraction for the cuvette is 100% as the whole beam overlaps with the sample. However, it is much lower for SCF as only a small fraction of the guided light is located outside of the glass core and in the holes. Only this fraction of the light is available for absorption measurement. The power fraction in the holes of the SCF with 1.5 μm core was calculated to be 1% via determining the difference between the loss of the fibre filled with water and the loss of the fibre filled with gold NP solution, and then dividing the difference by the loss value of the corresponding cuvette measurement.

Setting the measured power at the output of a fibre filled with water as 100%, we consider a decrease in transmission to 95% at the output of the same fibre filled with gold NP solution as the smallest transmission decrease that can be detected reproducibly. The corresponding absorbance value for this transmission decrease ($A = \log_{10}(100/95) = 0.0223$) is considered to be the LOQ. Therefore, this value was used to calculate either the fibre length to detect 100 ppb gold concentration, or the gold concentration that can be detected with 1 m of fibre (Table 2). These calculations demonstrate that for a LOQ of 100 ppb gold, fibre lengths of tens of metres are required. However, such fibre lengths are impractical due to long filling time. Using a shorter fibre length of 1 m increases the gold LOQ to >1 ppm. These best case scenario calculations indicate that absorption measurement with such an SCF having relatively low power fraction (~1%) in the holes cannot be used for field deployable sensors to detect sub-ppm gold concentrations.

The power fraction in the holes of a SCF increases with decreasing core size [42]. Therefore, use of SCF with smaller core size promises higher sensitivity due to enhanced light-matter overlap. However, core sizes <1 μm lead to increasing fibre loss and decreasing coupling efficiency unless more sophisticated coupling arrangements are used such as tapered couplers [41].

3.3. Fluorescence measurement in cuvette for detection of gold NPs

Fluorophore I-BODIPY resulted in a fluorescence peak at 510 nm in the presence of gold NPs, whereby the intensity of the peak increased with increasing concentration of gold NPs in the solution (Fig. 8). The observation of such a fluorescence peak is consistent with the results reported by Park et al. for a similar BODIPY derivative [28]. Using the laboratory spectrometer and cuvette measurements, we investigated the impact of incubation time and BODIPY concentration on the fluorescence intensity and hence the LOQ of 5 nm, 20 nm and 50 nm gold NPs.

Fig. 9 shows the impact of incubation time on the fluorescence intensity. For 20 nm and 50 nm gold NPs and all gold concentrations investigated, the peak fluorescence intensity increased until approximately 50 min and then saturated, indicating that after 50 min equilibrium for the transformation of I-BODIPY into H-BODIPY was reached. For 5 nm gold NPs even after 60 min no clear saturation was observed, indicating that the reaction rate for small NPs (5 nm) is slower than that for larger NPs (20 nm, 50 nm). The higher concentration of 5 nm gold NPs for the same weight ratio compared to the larger NPs (Table 3) requires longer time for the interactions between the NPs and the fluorophore. Due to the time dependence, the fluorescence intensity of the samples should be measured at the same incubation time, preferably after 50 min of incubation.

The investigations of a range of BODIPY concentrations (1 nM–500 nM) revealed that 60 nM was optimal as the fluorescence intensity was the highest (data not shown). Thus, for I-BODIPY concentration of 60 nM and incubation time of 50 min, the gold concentration dependence of fluorescence intensity was measured in cuvette using laboratory spectrometer (Fig. 10A) and portable spectrometer (Fig. 10B) for 5 nm, 20 nm and 50 nm gold NPs. The experimental LOQ of these measurements are depicted in Fig. 11. The LOQ of cuvette measurements using a portable

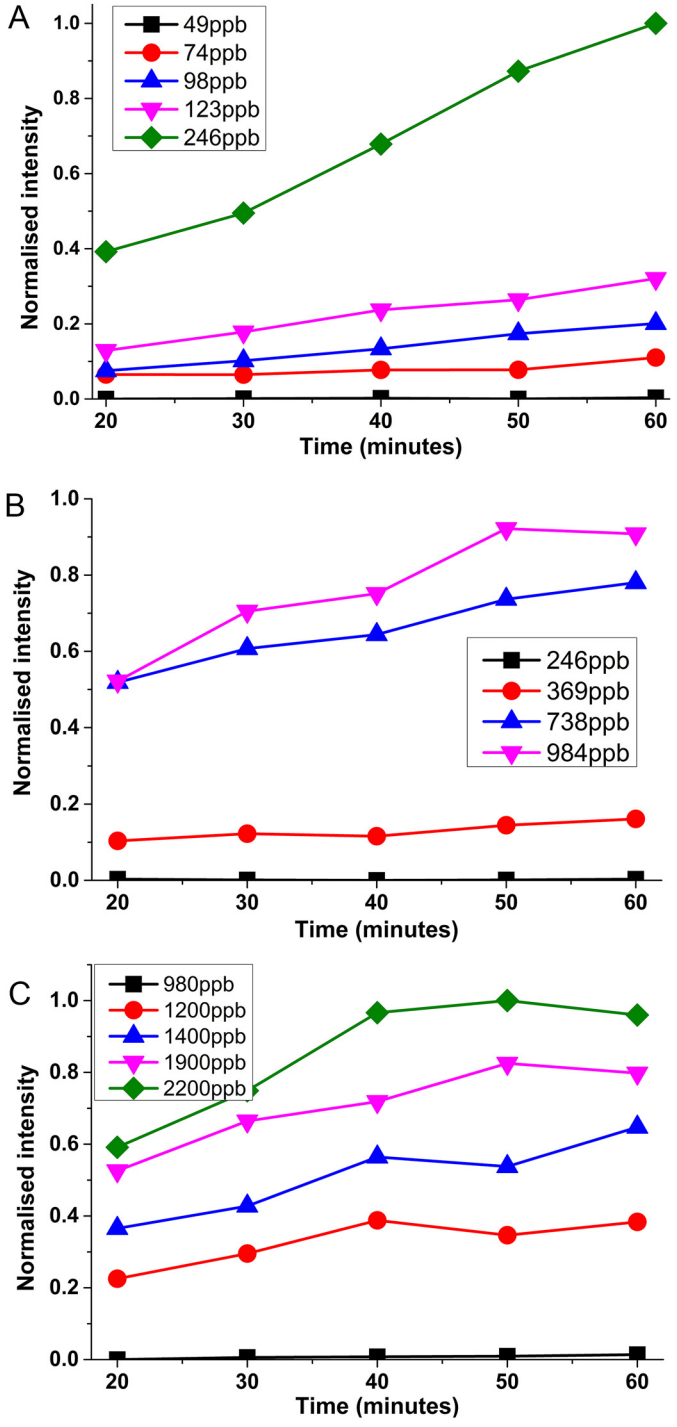

Fig. 9. Impact of incubation time on the fluorescence intensity for a range of gold concentrations measured in cuvette using laboratory spectrometer and 5 nm (A), 20 nm (B) and 50 nm (C) NPs mixed with 60 nM I-BODIPY.

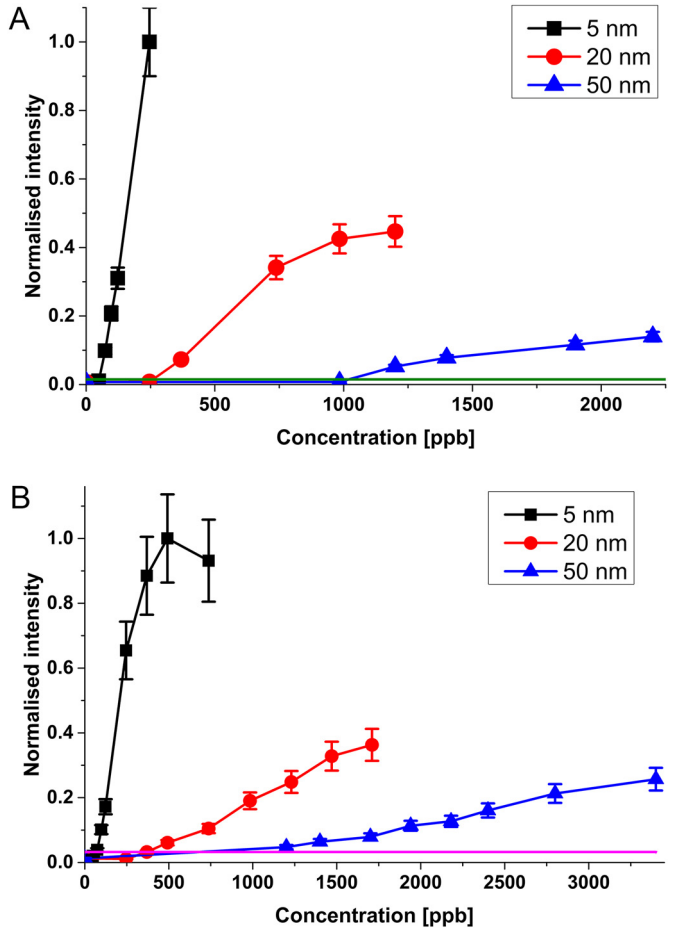

Fig. 10. Dependence of the fluorescence intensity at 510 nm on the gold concentration for 5 nm, 20 nm and 50 nm gold NPs at 50 min of incubation with 60 nM I-BODIPY measured in cuvette using (A) laboratory spectrometer and (B) portable spectrometer.

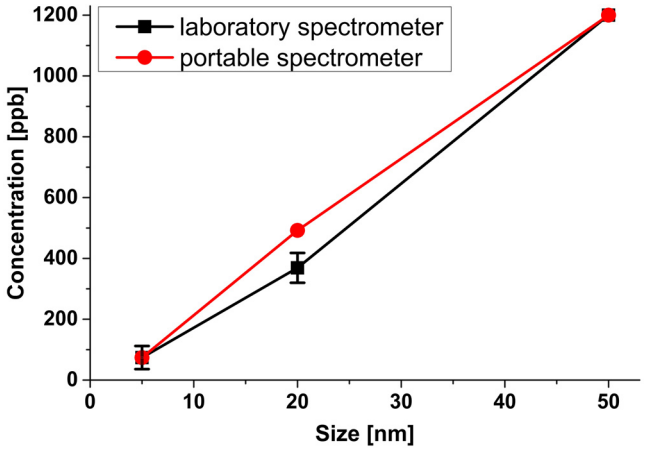

Fig. 11. LOQ for different sized gold NPs in a cuvette based on fluorescence measurements using 50 min incubation time and 60 nM I-BODIPY concentration for laboratory and portable spectrometer.

spectrometer was found to be identical to that using a laboratory spectrometer for 5 nm (74 ppb) and 50 nm (1200 ppb) NPs and slightly higher for 20 nm NPs (492 ppb and 392 ppb, respectively). The same or similar LOQ achieved for fluorescence studies using two different spectrometers is related to the same optical set up, and thus the same amount of laser light coupled into the sample and the same method of collection of fluorescent light measured. The consistent LOQ is also reflected in the similar LOQ obtained for both spectrometers (0.015 for laboratory spectrometer and 0.032 for portable one). The experimental values are lower than the theoretical values presented in Table 3 due to the range of analysed concentrations. The theoretical values lie between the experimental concentrations that are just below and just above the LOQ.

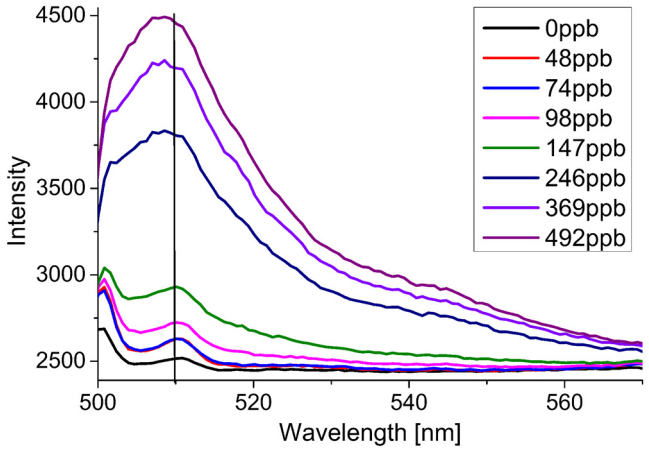

Fig. 12. Fluorescence spectra of an SCF filled with I-BODIPY and I-BODIPY with 5 nm gold NPs recorded with high resolution spectrometer. The peak at 510 nm (marked with black line) depends on the gold NP concentrations used.

3.4. Fluorescence measurement in fibre for detection of gold NPs

Fig. 12 shows the fluorescence spectra of SCF filled with I-BODIPY and different gold concentrations of 5 nm gold NPs after 50 min incubation time with 60 nM I-BODIPY using laboratory spectrometer. These fluorescence spectra indicate that measurements in an SCF yield similar results as for measurements in a cuvette.

The gold concentration dependence of the fluorescence intensity in an SCF was measured using different NP sizes at 50 min incubation time with 60 nM I-BODIPY for both laboratory and portable spectrometers (Fig. 13). The experimental LOQs for these measurements are: laboratory spectrometer—74 ppb for 5 nm NPs, 492 ppb for 20 nm NPs, 738 ppb for 50 nm NPs; portable spectrometer—74 ppb for 5 nm NPs, 246 ppb for 20 nm NPs and 492 ppb for 50 nm NPs. The results demonstrate that the LOQ in the SCF are similar for the two spectrometers used, which is consistent with the fluorescence measurements in the cuvette. There is some difference between the LOQ using the laboratory and portable spectrometers for 20 nm NPs (492 ppb and 246 ppb, respectively) and 50 nm NPs in fibre (738 ppb and 492 ppb, respectively) and no difference for 5 nm NPs (74 ppb). As explained above, similar LOQ regardless of the type of spectrometer used is related to the same optical set up used for the measurements and is reflected in similar value of spectrometer LOQ (0.059 for the laboratory spectrometer and 0.025 for the portable spectrometer). The experimental values differ from the theoretical values presented in Table 3 due to the range of analysed concentrations and error bars.

3.5. Fluorescence measurement: Impact of gold NP size on LOQ

Both cuvette and fibre studies show that the LOQ of fluorescence measurements decreases with decreasing gold NP size. This phenomenon is attributed to the different number of gold NPs in samples with the same gold concentration. For example, for the same gold concentration of 74 ppb, the NP concentration is higher for 5 nm NPs (97 pM) compared to 50 nm NPs (0.097 pM). The catalytic effect of gold NPs is expected to increase with increasing amount of NPs in a certain sample volume as then more gold NPs would be available to react with I-BODIPY. Conversion of the measured LOQ in molar concentration of gold NPs (Table 3) reveals that the LOQ in fact decreases with increasing gold NP size. The conversion also shows that for all NP sizes the molar NP concentration at LOQ is considerably smaller than that of I-BODIPY, which is consistent with the gold NPs acting as catalyser for the reaction of I-BODIPY to H-BODIPY.

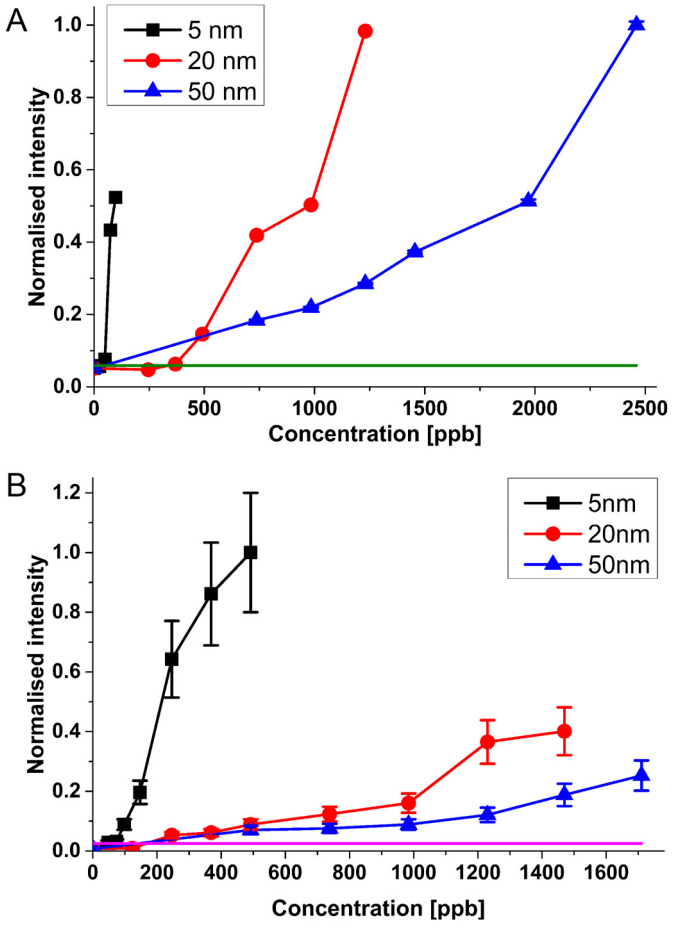

Fig. 13. LOQ for the three different sizes of gold NPs (5 nm, 20 nm, 50 nm) measured in an SCF using (A) laboratory spectrometer and (B) portable spectrometer.

The lower LOQ for 50 nm NPs measured in SCF compared to cuvette measurement is attributed to the interactions between gold NPs and the silica core of the fibre. For small NPs the repulsion forces are stronger than for bigger NPs [49]. It means that 50 nm NPs attach to the fibre core and interact with light longer than 5 nm NPs do, resulting in decreased LOQ in a fibre in contrast to cuvette.

Park [28] reported that BODIPY allows detection of gold NPs at NP concentrations as low as 500 pM (around 30 nm). We measured lower gold NP LOQ for all three NP sizes investigated, e.g. for measurements in an SCF using a laboratory spectrometer: 97.3 pM for 5 nm NPs, 10.1 pM for 20 nm NPs and 0.97 pM for 50 nm NPs. One possible reason for the difference in the LOQ between Park's and our results is the 17 times lower concentration of I-BODIPY used in our work. Other possible reasons are that we used a different derivative of I-BODIPY (lack of 3,5-bis(2-(2-(2-methoxyethoxy)ethoxy)ethoxy group on phenyl ring) as well as water as a solvent instead of ethanol:water 1:1 v/v.

Using an optical fibre decreases twice the LOQ for 50 nm NPs in comparison to measurements in a cuvette. This observation provides insight into the behaviour of the gold NPs and the fluorophore in different sensing chambers. Apart from the influence of the optical fibre on the LOQ, it also provides other benefits such as potential remote sensing and low volume of the sample, which is especially important for real world applications.

3.6. On-site gold detection

The LOQ for gold using current portable devices, such as a portable XRF (LOQ of 10 ppm) [23] is significantly above background (average crustal abundance of 1.3 ppb) [20] and above economic grades (~0.5–8 ppm) [21,22]. Thus, measuring the concentration of gold at the drill rig requires low LOQ and a portable set-up. The results shown here demonstrate that gold concentrations at ppb level usually detected using laboratory based spectrometer can be detected using portable spectrometers (Table 3). The LOQs for gold reported here are also well below economic values, and shows the potential in being able to detect anomalous gold concentrations that are significantly above background (average crustal abundance) and within the range of what would be desired for measuring gold in an exploration environment. However, the size of the NPs needs to be considered. Portable fluorescence analysis would give lower LOQ for small NPs, and the absorption method would allow lower LOQ of larger NPs. A fast method of synthesis of NPs of desirable size from drilling fluid will be the subject of the future paper.

Biological studies could also benefit from the portable detection of gold. Gold NPs 10–15 nm has been shown to pass through blood–brain barrier [18]. The accumulation of gold NPs as low as few ng/g (ppb) of animal has been shown e.g. in blood, bone and muscle [18]. These gold NP concentrations are within the detection range achievable with the methods described in this paper. Gold NPs conjugated with ligands such as antibody that binds specifically to a target, e.g. protein or cancer cell, could be collected with a blood sample or tissue biopsy and centrifuged to separate tissue from NPs. Quick analysis would lead to faster diagnosis of proteopathies or carcinogenesis.

4. Conclusion

The LOQ of gold NPs of different sizes has been defined for both absorption and fluorescence measurement methods using cuvette and SCF as well as laboratory and portable spectrometers for gold concentration in ppb and molar NP concentration in pM (Table 3).

The absorption LOQ in a cuvette measured with a laboratory Cary spectrometer was 7 times lower (dependent on NP size) than that measured with a portable spectrometer, which correlates with the approximately four times lower mean of blank sample (water) measured for the laboratory spectrometer. Absorption measurements in a SCF are impractical due to the long fibre length required for sub-ppm LOQs.

In contrast to the absorption method, the LOQ of the fluorescence method was approximately the same for both the laboratory Horiba and the portable spectrometer. This observation is related to the similar LOQ determined for both spectrometers. Our results suggest that LOQ values for laboratory Horiba and portable spectrometers are similar, while the laboratory Cary spectrometer allows the most sensitive analysis. However, note that the spectrometers were used in different set-ups and different types of blank samples were used. Comparing cuvette and SCF measurements, the LOQ was almost two times lower in the SCF for 50 nm NPs, but comparable for 5 nm and 20 nm NPs. It can also be noted that absorption method allows achieving lower LOQ than fluorescence in SCF for 50 nm NPs.

Considering gold concentration, larger NPs result in lower absorption LOQs but higher fluorescence LOQs. Conversely, considering gold NP concentration, bigger NP size leads to lower LOQs for both the absorption and the fluorescence methods.

The gold concentration based LOQs determined in this work using portable spectrometer demonstrate that a portable set-up can be used for on-site estimation of the presence of gold NPs. However the size of the NPs needs to be taken into account. Portability is an option for fluorescence analysis of gold NPs with low LOQ especially for small NPs (5 nm), while absorption measurement enables lower detection of larger NPs (50 nm).

Acknowledgements

This work was performed in part at the OptoFab node of the Australian National Fabrication Facility utilizing Commonwealth and SA State Government funding.

The work has been supported by the Deep Exploration Technologies Cooperative Research Centre whose activities are funded by the Australian Government's Cooperative Research Centre Programme. This paper is DET CRC report 2015/731.

We wish to acknowledge Dr Matthew Henderson for his help with an optical set up, Dr Herbert Foo for useful discussion and Dr Shahraam Afshar for providing the picture of light guided from the core to the holes of the fibre.

Appendix A. Supplementary data

Supplementary data associated with this article can be found, in the online version, at http://dx.doi.org/10.1016/j.snb.2015.12.044.

References

[1] M. Andrews, Australia's Paydirt, World gold council, 2013, pp. 38.
[2] B. Mukherji, E. Erhereine, Wall Street J. (2014).
[3] P. Guj, R. Schodde, Aust. Ins. Min. Metall. Bull. 2013 (3) (2013) 76–82.
[4] R.R. Hillis, D. Giles, et al., Soc. Econ. Geol. Spec. Publ. 18 (2014) 243–256.
[5] T. Poustie, P. Abbot, MESA J. 40 (2006) 4–7.
[6] M. Lintern, R. Anand, C. Ryan, D. Paterson, Nat. Commun. 4 (2013) 1–7, http://dx.doi.org/10.1038/ncomms3614, Article number: 2274.
[7] F. Reith, B. Etschmann, et al., Proc. Nat. Acad. Sci. U.S.A. 106 (42) (2009) 17757–17762.
[8] F. Reith, S.L. Rogers, D.C. McPhail, D. Webb, Science 313 (5784) (2006) 233–236.
[9] S. Parveen, R. Misra, S.K. Sahoo, Nanomed. Nanotechnol. Biol. Med. 8 (2) (2012) 147–166.
[10] S. Rana, A. Bajaj, R. Mout, V.M. Rotello, Adv. Drug Delivery Rev. 64 (2) (2012) 200–216.
[11] K. Saha, S.S. Agasti, C. Kim, X. Li, V.M. Rotello, Chem. Rev. 112 (5) (2012) 2739–2779.
[12] J. Conde, A. Ambrosone, et al., ACS Nano 6 (9) (2012) 8316–8324.
[13] J.J. Storhoff, S.S. Marla, et al., Biosens. Bioelectron. 19 (8) (2004) 875–883.
[14] J. Gao, X. Huang, H. Liu, F. Zan, J. Ren, Langmuir 28 (9) (2012) 4464–4471.
[15] L.C. Kennedy, L.R. Bickford, et al., Small 7 (2) (2011) 169–183.
[16] J.F. Hainfeld, M.J. O'Connor, et al., PLoS ONE 9 (2) (2014) e88414.
[17] Y. Pan, S. Neuss, et al., Small 3 (11) (2007) 1941–1949.
[18] N. Khlebtsov, L. Dykman, Chem. Soc. Rev. 40 (3) (2011) 1647–1671.
[19] J.S. Bozich, S.E. Lohse, et al., Environ. Sci.: Nano 1 (3) (2014) 260–270.
[20] R.L. Rudnick, S. Gao, in: H.D. Holland, K.K. Turekian (Eds.), Treatise on Geochemistry, Elsevier Ltd., Pergamon, Oxford, 2003, pp. 1–64.
[21] A.G. Tomkins, J.A. Mavrogenes, Econ. Geol. 97 (2002) 1249–1271.
[22] A. Belperio, R. Flint, H. Freeman, Econ. Geol. 102 (2007) 1499–1510.
[23] Olympus, 2015, from ⟨www.olympus-ims.com⟩ (accessed May 2015).
[24] ALS Geochemistry, Schedule of Services and Fees, ALS Limited, 2014.
[25] Intertek Genalysis Laboratory Services, Schedule of Services and Charges, Intertek Group plc, 2014.
[26] SGS, Fire assay gold, in: SGS Mineral Services, SGS Australia, 2013.
[27] B. Sciacca, T.M. Monro, Langmuir 30 (3) (2014) 946–954.
[28] J. Park, S. Choi, T.I. Kim, Y. Kim, Analyst 137 (19) (2012) 4411–4414.
[29] S. Mühlig, C. Rockstuhl, et al., Opt. Express 19 (10) (2011) 9607–9616.
[30] S. Zeng, X. Yu, et al., Sens. Actuators, B: Chem. 176 (0) (2013) 1128–1133.
[31] P.K. Jain, K.S. Lee, I.H. El-Sayed, M.A. El-Sayed, J. Phys. Chem. B 110 (14) (2006) 7238–7248.
[32] W. Haiss, N.T.K. Thanh, J. Aveyard, D.G. Fernig, Anal. Chem. 79 (11) (2007) 4215–4221.
[33] X. Liu, M. Atwater, J. Wang, Q. Huo, Colloids Surf., B: Biointerfaces 58 (1) (2007) 3–7.
[34] S. Heng, A.M. Mak, D.B. Stubing, T.M. Monro, A.D. Abell, Anal. Chem. 86 (2014) 3268–3272.
[35] S. Korposh, et al., Analyst 139 (2014) 2229–2236.
[36] R. Verma, B.D. Gupta, Analyst 139 (2014) 1449–1455.
[37] F. Chu, G. Tsiminis, N.A. Spooner, T.M. Monro, Sens. Actuators, B: Chem. 199 (0) (2014) 22–26.
[38] S.C. Warren-Smith, S. Heng, H. Ebendorff-Heidepriem, A.D. Abell, T.M. Monro, Langmuir 27 (9) (2011) 5680–5685.

[39] E.P. Schartner, H. Ebendorff-Heidepriem, S.C. Warren-Smith, R.T. White, T.M. Monro, Sensors 11 (3) (2011) 2961–2971.
[40] C. Zhang, et al., J. Am. Chem. Soc. 135 (2013) 10566–10578.
[41] H. Ebendorff-Heidepriem, S.C. Warren-Smith, T.M. Monro, Opt. Express 17 (2009) 2646–2657.
[42] S.C. Warren-Smith, S. Afshar, T.M. Monro, Opt. Express 18 (9) (2010) 9474–9485.
[43] J. Inezedy, T. Lengyel, A. Ure, Compedium on analytical nomenclature. Definitive roles, in: International Union of Pure and Applied Chemistry, third ed., 1997, ⟨http://www.iupac.org/publications/analytical_compendium/⟩.
[44] D. Tholen, K. Linnet, et al., NCCLS Doc. 24 (34) (2004) 1–39.
[45] Nanocomposix, 2015, ⟨http://nanocomposix.com/collections/silver⟩.
[46] W.L. Barnes, A. Dereux, T.W. Ebbesen, Nature 424 (6950) (2003) 824–830.
[47] M.A.K. Abdelhalim, M.M. Mady, M.M. Ghannam, J. Nanomed. Nanotechnol. 3 (3) (2012) 1–5.
[48] T.G. Euser, J.S.Y. Chen, et al., J. Appl. Phys. 103 (10) (2008) 103108.
[49] Y. Min, M. Akbulut, K. Kristiansen, Y. Golan, J. Israelachvili, Nat. Mater. 7 (7) (2008) 527–538.

Biographies

Agnieszka Zuber completed her PhD at Mawson Institute, University of South Australia in 2013. The subject of her research was a development of a graft for intraocular transplantation. She joined Institute for Photonics and Advanced Sensing in 2013. She was working on the development of the sensor for detection of the proteins related to early stage of gastric cancer. Currently she is working with the Deep Exploration Technologies CRC on the detection of gold for mining industry.

Malcolm Purdey completed a Bachelor of Science at The University of Adelaide with majors in chemistry and pharmacology in 2010. In 2011 he completed Honours in amyloid inhibitor peptide chemistry. He is now studying a PhD under supervision of Prof. Andrew Abell, Prof. Tanya Monro and Prof. John Carver working on sensing of hydrogen peroxide using fluorophores.

Erik Schartner completed his PhD on a collaborative project with The Defence Science and Technology Organisation on a project entitled "Hydrogen peroxide sensing with microstructured optical fibres: fuel, wine and babies." Since the completion of his PhD Erik has worked on a linkage project with Cook Medical, on the development of novel optical fibre probes for measurements of pH and temperature in the local medium surrounding embryos. He is currently working as a Research Fellow in the Centre for Nanoscale Biophotonics, looking at the deployment of novel optical fibre sensors in bioapplications.

Caroline Forbes received her PhD degree from Monash University in 2006. She is a geoscientist and has research interests in geochemistry, tectonics and resource geology. She currently working with the Deep Exploration Technologies CRC on developing new drilling technologies for hard rock mineral exploration, and on understanding geochemical footprints in cover and basement rocks associated with iron oxide-copper-gold deposits.

Benjamin van der Hoek completed his PhD on a project entitled "Regolith expressions of concealed gold mineralisation in the central Gawler Craton, South Australia" in 2014. He is working as a geologist/geochemist with the Deep Exploration Technologies CRC on the project investigating the workflow and geological sample quality when drilling with a Coiled Tube drill rig, and the subsequent real-time geochemical and mineralogical analysis of the samples.

David Giles, professor at the University of Adelaide, completed his PhD at Monash University in 2000. Between 2003 and 2006 he was chief investigator on an ARC Linkage Project, in collaboration with BHP Billiton, concerned with the development of base metal mineral deposits in Proterozoic basins. He is the State of South Australia Chair of Mineral Exploration and Director of the Centre for Mineral Exploration Under Cover (CMXUC) at the University of Adelaide. As Deep Exploration Technologies CRC program leader he is working on a development of new technologies for mapping of the mineral systems for exploration.

Andrew Abell graduated from the University of Adelaide with a PhD and then undertook a postdoctoral fellowship at the University of Cambridge. He accepted a lectureship at the University of Canterbury in 1987 and was subsequently promoted to Professor. He has supervised in excess of 75 postgraduate and honours students and 30 post-doctorial fellows over the last 15 years. The results of his research have been published in more than 200 international publications. He is Adelaide node leader for the ARC Centre of Excellence for Nanoscale Biophotonics. His research focuses on the design, synthesis, and exploitation of small molecule enzyme inhibitors and mimics of key biological compounds as a basis of new therapeutics for cancer and other diseases as well as probes to study key metabolic processes such as electron transfer.

Tanya Monro, professor at The University of Adelaide, obtained her PhD in physics in 1998 from The University of Sydney, for which she was awarded the Bragg Gold Medal for the best Physics PhD in Australia. In 2000, she received a Royal Society University Research Fellowship at the Optoelectronics Research Centre at the University of Southampton in the UK. She came to the University of Adelaide in 2005 as inaugural Chair of Photonics. Tanya was the inaugural Director of the Institute for Photonics and Advanced Sensing from 2008 to 2014 and was also the inaugural Director for the ARC Centre of Excellence for Nanoscale BioPhotonics at the University of Adelaide. She has published over 500 papers in refereed journals and conference proceedings. Currently, she is Deputy Vice Chancellor Research and Innovation and an ARC Georgina Sweet Laureate Fellow at the University of South Australia.

Heike Ebendorff-Heidepriem is professor at the University of Adelaide. She received the PhD degree in chemistry from the University of Jena (Germany) in 1994, where she continued her research on optical glasses until 2000. During 2001–2004, she was with the Optoelectronics Research Centre at the University of Southampton, working on novel photosensitive glasses and soft glass microstructured optical fibres with record optical nonlinearity. Since 2005, she has been with The University of Adelaide, Australia. Currently, she is deputy director of the Institute for Photonics and Advanced Sensing. Her research focuses on the development of mid-infrared, high-nonlinearity, active and nanocomposite glasses; glass, preform and fibre fabrication techniques and surface functionalisation of glass. Heike has published over 170 refereed journal papers and conference proceedings including 16 review papers.